Sequestration of Radionuclides Radium-226 and Strontium-90 by Cyanobacteria Forming Intracellular Calcium Carbonates

Neha Mehta, Karim Benzerara, Benjamin Kocar, Virginie Chapon

Sequestration of radionuclides Radium-226 and Strontium-90 by cyanobacteria forming intracellular calcium carbonates

Neha Mehta[1], Karim Benzerara[2*], Benjamin D. Kocar[1,3*], Virginie Chapon[4]

[1,3] Department of Civil and Environmental Engineering, Massachusetts Institute of Technology, Cambridge, Massachusetts 02139, United States

[2] Sorbonne Université, Muséum National d'Histoire Naturelle, UMR CNRS 7590, Institut de Minéralogie, de Physique des Matériaux et de Cosmochimie, IMPMC, 75005 Paris, France

[3.] Exponent, Inc. 1055 E. Colorado Blvd, Suite 500. Pasadena, California 91106, United States.

[4] CEA, CNRS, Aix-Marseille Université, UMR 7265 Biosciences and Biotechnologies Institute of Aix-Marseille, 13108 Saint-Paul-lez-Durance, France.

*Corresponding Authors

Email: bkocar@exponent.com; karim.benzerara@sorbonne-universite.fr

ABSTRACT: ^{226}Ra is a naturally occurring radionuclide with a half-life of 1600 y. In contrast, ^{90}Sr is a radionuclide of sole anthropogenic origin, produced by nuclear fission reactions and has a half-life of 29 y; each of these radionuclides poses potential threats to human and ecosystem health. Here, the cyanobacterium *G. lithophora,* capable of forming intracellular amorphous calcium carbonate inclusions, was investigated for its ability to uptake ^{226}Ra and ^{90}Sr. In BG-11 medium, *G. lithophora* accumulated 3.9 µg g^{-1} ^{226}Ra within 144 h and 47.9 ng g^{-1} ^{90}Sr within 1 h, corresponding to ~99% removal of trace radionuclides. The presence of high concentration Ca^{2+} in the background media solution did not inhibit ^{90}Sr and ^{226}Ra uptake by *G. lithophora*. In contrast, dead biomass of *G. lithophora* accumulated 0.8 µg g^{-1} ^{226}Ra and 8.87 ng g^{-1} ^{90}Sr. Moreover, *Synechocystis,* a non-biomineralizing cyanobacteria removed only 14% and 25% of ^{226}Ra and ^{90}Sr, respectively. This suggested that sequestration of ^{90}Sr and ^{226}Ra was not intrinsic to all cyanobacteria but was likely a specific biological trait of *G. lithophora* related to the formation of intracellular amorphous Ca-carbonates. The unique ability of *G. lithophora* to uptake ^{90}Sr and ^{226}Ra at

high rates makes it an attractive candidate for further studies involving bioremediation of these radionuclides.

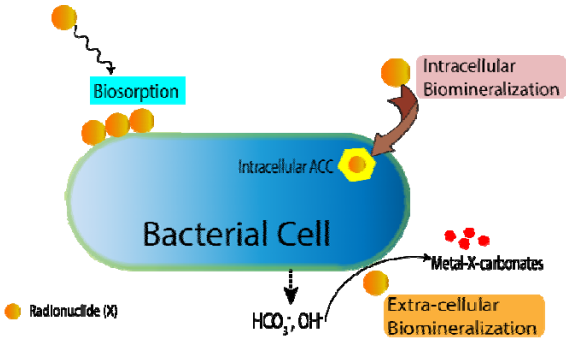

TOC image

1. Introduction

Cyanobacteria are a phylogenetically and ecologically diverse group of photosynthetic bacteria, playing a vital role in the global cycling of numerous elements such as carbon (C), calcium (Ca) and phosphorus (P)[1]. In particular, their impact on the global carbon cycle is of significant interest as they sequester atmospheric CO_2 into organic carbon and biogenic calcium carbonates ($CaCO_3$) through calcification[2]. In cyanobacteria, this process has long been considered as extracellular and non-biologically controlled. However, this paradigm was challenged by the recent discovery of several species of cyanobacteria forming intracellular amorphous calcium carbonate (ACC) inclusions in very diverse environments.[3] Couradeau *et al.* first described this intracellular calcification in the cyanobacterium *Gloeomargarita lithophora,* isolated from an alkaline freshwater lake Alchichica microbialite, Mexico[4]. These ACC inclusions measured several hundreds of nanometers in diameter, were poorly crystalline and were composed of CO_3 and Ca-Mg-Sr-

Ba, with Ba/Ca and Sr/Ca atomic ratios in inclusions higher by factors of 1370 and 90 respectively relative to the solutions in which cells grew [3,4]. Recently, it was confirmed that cyanobacteria capable of forming intracellular ACC contained a much higher content of alkaline earth elements (AEE) than all other cyanobacteria[5]. In addition to intracellular ACC inclusions, *G. lithophora* also forms intracellular polyphosphate inclusions (PolyP), polymers of orthophosphate which may serve as reserves of P and/or energy for cells[6]. Using stable isotopes, Cam *et al*. showed that *G. lithophora* preferentially accumulated Ba over Sr and finally Ca within intracellular PolyP and ACC. Currently, the origin of such a surprising selectivity remains unclear. The proven ability of *G. lithophora* to selectively sequester Sr over Ca within intracellular inclusions provides an intriguing microbial framework to examine if this ability extends to radioactive AEE such as radium (^{226}Ra) and radio-strontium (^{90}Sr). In the environment, ^{90}Sr and ^{226}Ra are present at trace concentrations, along with excess dissolved Ca. Whether the observed selective accumulation of AEE is extended to ^{90}Sr and ^{226}Ra at such low concentrations and in the presence of high concentrations of Ca remains to be explored.

Radium-226 is a naturally occurring radioactive alkaline earth element (AEE) with a half-life of 1600 y. It is one of the dominant soluble radionuclides present in groundwater[7]. In the United States, ^{226}Ra activity in drinking water is regulated at 0.2 Bq L^{-1} [8]. Potential exposure to Ra could originate from the disposal and management of large volumes of Ra-bearing waste streams associated with uranium mining, phosphate mining and milling operations, coal mining and power plants, and conventional and unconventional oil and gas extraction[9]. The Ra content of these waste streams can range from 100-1200 Bq L^{-1}, which far exceeds the regulatory limit of 2.2 Bq L^{-1} Ra in effluent waste stream[10]. During disposal

and storage of relatively large volumes of these streams, leaching of Ra (and other toxic elements) could result in contamination of terrestrial and subsurface aquatic environments[11,12].

In contrast, radio-Strontium (^{90}Sr) is a radionuclide of sole anthropogenic origin produced by nuclear fission reactions. With its long half-life of 29 years, ^{90}Sr persists sufficiently long in the environment to warrant health concerns. The main sources of ^{90}Sr in the environment are the atmospheric tests of nuclear weapons conducted from 1945 to 1980's and nuclear accidents, such as Fukushima and Chernobyl[13,14]. Measured ^{90}Sr specific activity in the surface waters adjacent to the Fukushima Daiichi Nuclear Power Plant varied between 0.2 - 400 kBq m^{-3}, which were about 4 orders of magnitude greater than the pre-accident level (1 Bq m^{-3})[15]. Strontium is very soluble, highly mobile and is bioavailable in the environment. Its soluble form, Sr^{2+} can be transferred from contaminated soils and water into living organisms through the food chain. A chemical analog of Ca^{2+}, $^{90}Sr^{2+}$ concentrates in bone tissues in the human body, increasing the probability of bone cancer after accumulation and prolonged exposure [16].

Several physiochemical strategies have been developed for decontamination of ^{226}Ra and ^{90}Sr from effluent waste streams. However, in many cases their application is limited due to economic constraints[17]. In addition, the presence of high concentrations of Ca and other co-contaminants often present within waste streams limits the selective removal of ^{226}Ra and ^{90}Sr using the traditional schemes[18,19]. On the other hand, bioremediation strategies are gaining significant interest owing to their relative cost-effectiveness and eco-friendliness[20–22]. Various types of organisms including fungi, algae, cyanobacteria, and phytoplankton have been reported to retain ^{226}Ra and ^{90}Sr[9,23]. Different pathways of

sequestration can be involved. ^{226}Ra and ^{90}Sr can adhere to the surface of living and dead cells. Ligands (carboxyl, amine, hydroxyl, phosphate, and sulfhydryl groups) present in the cell membrane of both Gram-positive and Gram-negative bacteria can bind positively charged metals through adsorption[24]. Some examples of such microorganisms adsorbing ^{226}Ra include dead microbial biomass of *Pseudomonas aeruginosa, Nostoc carneum, Nostoc insulare, Oscillatoria geminanat, Spirullina laxissima, Pseudomonas fluorescens*, *Streptomyces nives,* and mixed bacterial cultures from activated wastewater sludges [23,25]. The dead biomass of bacterial strains isolated from areas with a high level of natural radiation, such as *Citrobacter freundii, Chromobacterium, Chryseobacterium,* and *Corynebacterium* also have been shown to adsorb ^{226}Ra[26]. In the case of ^{90}Sr, studies have often been performed using stable Sr isotopes to examine the ^{90}Sr remediation potential of an organism. Some organisms such as the algae *Scenedesmus spinosus* and *Oedogonium* sp. *Nak 1001,* the cyanobacteria *Oscillatoria homogenea* and *Stigonema ocellatum* NIES-2131, and the aquatic plant *Egeria densa* We2 have been reported to show high stable-Sr adsorption[27,28]. In addition to adsorption, many types of microorganisms may accumulate ^{226}Ra and ^{90}Sr within extracellularly or intracellularly precipitated biogenic minerals. The formation of biominerals occurs in response to localized changes in cellular or extracellular microenvironments. To our knowledge, there is no known micro-organism which has been reported to biomineralize ^{226}Ra. Several organisms have been screened for their ability to (co)-precipitate Sr. For example, the microalga *Chlorella vulgaris,* soil bacterium *Sporosarcina pasteurii* and the bacterium *Halomonas* sp. induce co-precipitation of strontianite ($SrCO_3$) within extracellularly precipitated $CaCO_3$ mineral phase; the desmid *Closterium moniliferum* forms celestite ($SrSO_4$) within its vacuole by concentrating

117 preferentially Sr and Ba over Ca[29–32]. More recently, Cam *et al*. showed stable-Sr is
118 selectively accumulated within intracellular ACC and PolyP inclusions in the
119 cyanobacterium *G. lithophora*[33]. Owing to selectivity for Sr compared to Ca, *G. lithophora*
120 forms carbonate with higher Sr content in comparison to other bacteria forming extracellular
121 carbonates. This means that the mass of the decontamination by products will therefore be
122 lower which may offer a cost advantage. Some of the non-photosynthetic bacteria which are
123 known to precipitate $CaCO_3$ efficiently, exhibit lower Sr removal efficiency in comparison
124 to *G. lithophora*. For example, *S. pasteurii* removes upto 59% of Sr from the solution
125 whereas *G. lithophora* removes 100% of Sr from the solution[32,33].

126 Despite screening of several organisms for removal of ^{90}Sr and ^{226}Ra, these studies
127 have not demonstrated their potential for use in bioremediation. Indeed, research on ^{90}Sr
128 bioremediation has mostly utilized stable-Sr isotope as an analog of ^{90}Sr and at relatively
129 high concentrations. Owing to the radiotoxicity of ^{90}Sr, it is unclear whether the results
130 demonstrated using stable Sr isotopes would be replicated to the same extent in presence of
131 ^{90}Sr. Further, ^{226}Ra and ^{90}Sr removed from solution through adsorption to biomass is prone
132 to rapid desorption upon changes in aqueous chemistry. Moreover, biomass is not selective
133 and other divalent cations (e.g. Ca, Ba), which are often present at relatively high
134 concentrations in ^{226}Ra and/or ^{90}Sr contaminated aqueous environments, may outcompete
135 ^{226}Ra and/or ^{90}Sr for binding sites, resulting in low removal efficiency[22,24]. Thus,
136 effectiveness of ^{226}Ra and ^{90}Sr bioremediation strategies will be dictated by (micro)-
137 organisms capability to selectively remove the radionuclide at trace concentration in the
138 presence of competing elements while also tolerating ionizing radiation.

Here, the role of the cyanobacterium *G. lithophora* forming intracellular biominerals on sequestration of ^{226}Ra and ^{90}Sr at trace concentrations is evaluated. We selected *G. lithophora* to evaluate as a potential bioremediation tool for removing ^{90}Sr and ^{226}Ra from solution for several reasons. Because of the photoautotrophic lifestyle of cyanobacteria, *G. lithophora* may exhibit tolerance to substantial levels of ionizing radiation[34]. Moreover, unlike other (micro)organisms, *G. lithophora* has been shown to preferentially sequester Sr over Ca within intracellular ACC and PolyP inclusions, despite their chemical similarity. These characteristics make *G. lithophora* a promising candidate for bioremediation of ^{226}Ra and ^{90}Sr. Proving the ability of *G. lithophora* to sequester ^{226}Ra and ^{90}Sr through a novel (co)-precipitation pathway will illustrate its promise for use in bioremediation efforts; also, owing to its widespread ecological distribution[35], its cultivability and the availability of its genome sequence[36], *G. lithophora* serves as an ideal model organism for examining underlying biochemical processes responsible for bioaccumulation of radioactive AEE in microbes. Accordingly, the goals of the current study are 1) to investigate and quantify ^{226}Ra and ^{90}Sr uptake by *G. lithophora* using laboratory batch incubations, and 2) to identify retention mechanism of ^{226}Ra and ^{90}Sr by *G. lithophora*.

2. EXPERIMENTAL SECTION:

Incubations and Culture Conditions

The cyanobacterial strain *G. lithophora* was obtained from Institut de Minéralogie, de Physique des Matériaux et de Cosmochimie, IMPMC, Paris, France and cultured in the BG-11 medium at 30° C under continuous light (5-10 µmol m^2 s^{-1}) as described by Moreira *et al.* [36]. The BG-11 medium contained $17.6x10^{-3}$ M $NaNO_3$, $0.23x10^{-3}$ M K_2HPO_4, $0.3x10^{-3}$ M $MgSO_4$, $2.5x10^{-4}$ M $CaCl_2$, $3.1x10^{-5}$ M citric acid, $2x10^{-5}$ M ferric ammonium citrate, $3x10^{-6}$ M ethylenediaminetetraacetic acid (EDTA), $5x10^{-4}$ M $NaHCO_3$, and trace metals[37]. The

optical density (OD) of the suspensions was measured at 730 nm; based on the previous work by Cam *et al.*[33], the relationships between OD, cell density and cell dry mass of *G. lithophora*, were estimated as 9 x 10^7 cells. mL^{-1} OD $unit^{-1}$ and 3.65 x 10^{-4} g of dry mass. OD $unit^{-1}$. mL^{-1}.

^{226}Ra uptake by G. lithophora

^{226}Ra uptake was measured during the growth stage of *G. lithophora* cultures, which were started at low cell density ($OD_{t=0}$=0.039± 0.01). Pre-cultures used for inoculation were centrifuged at 5000 g for 15 min and the cell pellets were re-suspended in BG-11 amended with ^{226}Ra and total Ca as chloride salts at concentrations of 7.5 x 10^{-10} M (*i.e.* 6153 Bq L^{-1} ^{226}Ra) and 6.32 x 10^{-4} M, respectively and buffered at pH 8 using HEPES buffer. Triplicate incubations were performed. Three types of controls were included in the experimental design:1) an abiotic control consisting of BG-11 medium amended with 7.5 x 10^{-10} M of ^{226}Ra and 6.32 x 10^{-4} M of Ca^{2+}. 2) Inactivated cells control consisted of *G. lithophora* cells cultured in BG-11, killed by gamma irradiation (^{60}Co source, 55 h) and re-suspended at an OD of 1 in fresh BG-11 medium with 5.2 x 10^{-10} M (*i.e.* 5600 Bq L^{-1}) of ^{226}Ra and 2.5 x 10^{-4} M of Ca^{2+}. This control was used to quantify ^{226}Ra uptake by dead *G. lithophora* biomass and adsorption of ^{226}Ra to walls of the culture vessel. 3) Living cells of *Synechocystis* sp. PCC 6803 (obtained from Pasteur Collection of Cyanobacteria) cultured in BG-11 and amended with 5.2 x 10^{-10} M (*i.e.* 5600 Bq L^{-1}) of ^{226}Ra and 2.5 x 10^{-4} M of Ca^{2+}. This species has been shown to be unable to biomineralize intracellular ACC[3]. The OD of *Synechocystis* sp. PCC 6803 cultures at the start of experiment was equal to 0.02 ± 0.002.

Dissolved Ca^{2+} concentration and residual ^{226}Ra activity in solution were measured in all solutions as a function of time. For dissolved Ca^{2+} measurements, 100 µl of the culture

were mixed with 2 ml of standard BG-11 medium and were filtered on 0.22 µm PES syringe filters. Filtrates were acidified with 3 mL of 3 % HNO_3. Dissolved Ca^{2+} concentrations were measured using an Agilent Inductively Coupled Optical Emission Spectrometer (ICP-OES). Concentration of Ca^{2+} was also measured in the reagent blank (2 mL BG-11 + 3 mL 3 % HNO_3) to eliminate background signal.

For measurement of residual ^{226}Ra in solution, 500 µl of the culture were mixed with 2 ml of standard BG-11 medium and were filtered on 0.22 µm PES syringe filters. Filtrates were acidified with 3% HNO_3 and counted using a Canberra High Purity Germanium Detector (HPGe) Gamma Spectrometer. Energy and efficiency calibration of gamma spectroscopy was performed using a mixed multi-nuclide Eckert & Ziegler™ aqueous gamma standard. ^{226}Ra was directly measured from its gamma peak at 186.5 keV.

^{90}Sr uptake by G. lithophora

^{90}Sr uptake by *G. lithophora* was studied following a different strategy. In this case, cell suspensions of *G. lithophora* at high cell density were used. The high cell density of the culture is expected to provide a faster uptake of ^{90}Sr. Cells previously grown in standard BG-11 to an OD of 1 were centrifuged at 8500 g for 10 min and the cell pellets were re-suspended in standard BG-11 at an OD of 0.5 (*i.e.* 0.1825 g L^{-1}). The suspensions were then amended with 8.8 x 10^{-11} M of ^{90}Sr (*i.e.* 4 x 10^4 Bq L^{-1}). Three types of controls were included in the experiment: 1) an abiotic control consisting of BG-11 medium amended with 8.8 x 10^{-11} M of ^{90}Sr. 2) Inactivated cells control consisting in *G. lithophora* cells grown in BG-11 medium, freeze-dried and killed by autoclaving (121 °C in 20 min). Dried biomass was suspended at 0.2 g L^{-1} in BG-11 amended with 8.8 x 10^{-11} M of ^{90}Sr. The protocol of cell inactivation was different in this case than for experiments with ^{226}Ra. However, both

approaches were similarly efficient at providing dead cell controls which eventually show low sorption capabilities of ^{226}Ra and ^{90}Sr as detailed later in the manuscript 3) Living cells of *Synechocystis* sp. PCC 6803 grown in BG-11, collected by centrifugation at 8500 g for 10 min, re-suspended in fresh BG-11 at an OD of 0.5 and amended with 8.8×10^{-11} M of ^{90}Sr.

Triplicate incubations were performed for all experimental treatments. Total ^{90}Sr and residual ^{90}Sr in solution were measured in all solutions after 0.5, 24 and 48 h incubation in the light. Temperature was maintained at 30°C within a MINITRON incubator (INFORS) with shaking at 100 rpm. For residual ^{90}Sr quantification, 1 mL of cell suspension was centrifuged at 8500 g for 10 min and the supernatant was filtered on a 0.22 µm PVDF syringe filter. The volume of the filtered supernatant was measured as 930 ± 2 µL. Two milliliters of scintillating solution (Ultima Gold™, PerkinElmer) were added to the filtrates before counting on a Tri-Carb® 3100TR low activity liquid scintillation analyzer (PerkinElmer). For total ^{90}Sr content quantification, 930 µL of cell suspension were mixed with 2 mL scintillating solution and counted. ^{90}Sr standard solutions were prepared with the ^{90}Sr stock solution (LEA, Pierrelatte, France), diluted in BG-11 medium and counted as described for the other samples. The counts per second (CPS) values were corrected from the background activity, measured with a control made of 930 µL of BG-11 medium and 2 mL scintillation solution. The concentration of ^{90}Sr (Bq L^{-1}) in the samples was derived from the standards.

Calculation of bioaccumulation of ^{90}Sr and ^{226}Ra

The mass of ^{90}Sr and ^{226}Ra accumulated by the cells at a time *t* and normalized by the cell mass was determined as follows:

For ^{226}Ra:

$$\frac{(X_0 - X_t)\alpha}{cell\ mass\ accumulated\ between\ 0\ and\ t}$$

and for ^{90}Sr:

$$\frac{(X_0 - X_t)\alpha}{cell\ mass\ at\ t}$$

where X denotes radionuclide activity (Bq L^{-1}), α is the factor to convert activity of a radionuclide to mass units and *t* is the sampling time. The value of α for ^{226}Ra and ^{90}Sr is equal to 1.2×10^{-13} (mol Bq^{-1}) and 2.2×10^{-15} (mol Bq^{-1}).

3. RESULTS AND DISCUSSION

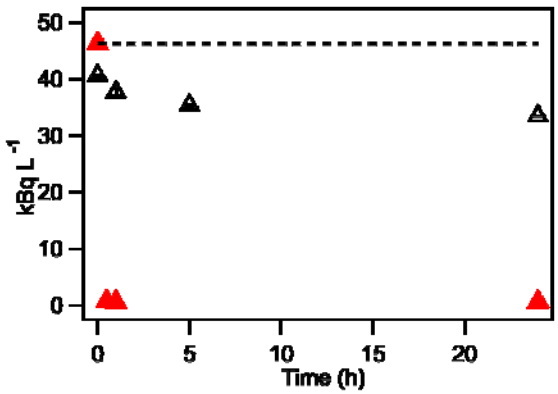

Figure 1: Time evolution of residual ^{90}Sr activity in the solution during exposure of *G. lithophora* cells to 8.8×10^{-11} M ^{90}Sr (▲) and in the abiotic control (Δ), both in BG-11. The dash lines denote the initial total activity of ^{90}Sr added to the cultures. When not visible, error bars are smaller than the symbols.

Kinetics of ^{90}Sr uptake by *G. lithophora*

In order to demonstrate the uptake of radionuclides by *G. lithophora*, we first monitored uptake of ^{90}Sr at high cell density to avoid any potential toxic effects on its growth by ^{90}Sr. The residual ^{90}Sr activity in solution during exposure of *G. lithophora* cells

to 8.8 x 10^{-11} M ^{90}Sr is shown in Figure 1. ^{90}Sr was rapidly removed from the solution in the presence of *G. lithophora*: the residual ^{90}Sr activity in the solution decreased from 46.243 ± 0.604 kBq L^{-1} to 0.753 ± 0.129 kBq L^{-1} within 1 h, corresponding to the sequestration of 98 % of the radionuclide by the cells. The presence of divalent ions (e.g. Ca^{2+}, Mg^{2+}) in solution did not inhibit ^{90}Sr uptake by *G. lithophora* cells, consistent with results obtained with stable Sr[33]. Following the observed rapid decline of the residual ^{90}Sr activity in the solution, the rate of ^{90}Sr uptake by *G. lithophora* decreased. At the end of incubation (48 h), the residual ^{90}Sr activity reached 0.608 kBq L^{-1}, corresponding to 99 % of radionuclide removal by the cells. Here, removal of ^{90}Sr by *G. lithophora* occurred from solutions containing a high concentration of Ca, with an initial Ca/^{90}Sr molar ratio of 2.7x10^{6}. Thus *G. lithophora* can efficiently sequester ^{90}Sr at trace concentrations despite the presence of a large excess of competing cations. Within abiotic controls, only 12% of ^{90}Sr was removed from solution within 5 hours, and ^{90}Sr activity remained constant thereafter for the duration of the experiment.

Kinetics of ^{226}Ra uptake by *G. lithophora*

Based on the promising uptake of ^{90}Sr exhibited by *G. lithophora* cells, the next step was to investigate whether the uptake of radiotoxic AEE could also occur during the growth

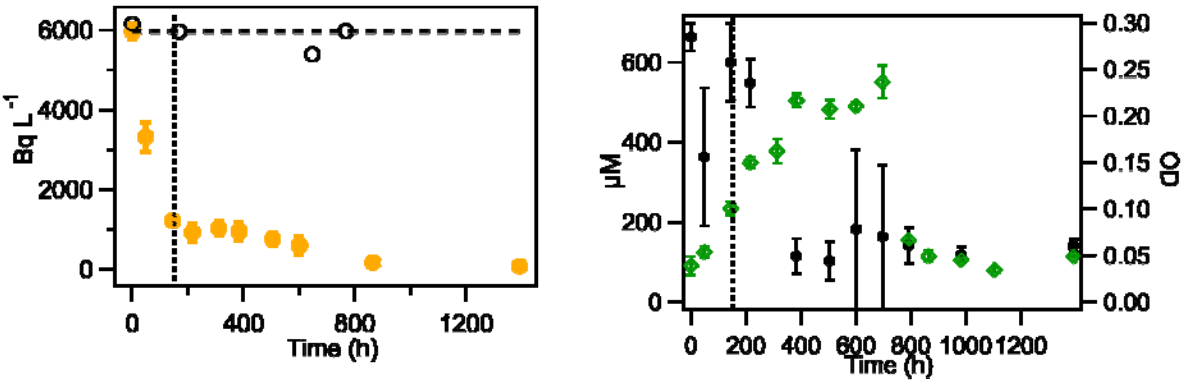

Figure 2: (Left) Time evolution of residual ^{226}Ra activity in the solution during growth of *G. lithophora* with 8 x 10^{-10} M ^{226}Ra (●) and in abiotic control (o), both in BG-11. Error bars denote the standard deviations of triplicate measurements. The horizontal dash line indicates the activity of ^{226}Ra added to the BG-11 media used for growing *G. lithophora*. (Right) Time evolution of dissolved Ca^{2+} (⬢) concentration and OD (◇) of cell suspension during growth of *G. lithophora* in BG-11 amended with 8 x 10^{-10} M ^{226}Ra. When not visible, error bars are smaller than the symbols, except for the abiotic control, for which triplicate measurements were not performed. The vertical dash line indicates the beginning of the second stage of ^{226}Ra uptake.

stage of *G. lithophora*. For this purpose, we measured ^{226}Ra uptake upon the growth of *G. lithophora* cells starting at a low cell density.

The uptake of ^{226}Ra by *G. lithophora* was examined within low-cell density cultures for reasons described above, and occurred in two stages (Figure 2, left). In the first stage, ^{226}Ra was rapidly removed from solution, with ^{226}Ra activity decreasing from 5964 ± 192.2 Bq L^{-1} to 1227.68 ± 85.5 Bq L^{-1} in 144 h. This removal was accompanied by a slight decrease in dissolved Ca^{2+} (Figure 2, right). In the second stage, the rate of removal of ^{226}Ra from the solution slowed down and residual ^{226}Ra activity in the solution further decreased to 82 Bq L^{-1}in 1392 h. The initial period of this 2nd stage was marked with an appreciable

271 decrease in dissolved Ca^{2+} in comparison to the 1st stage. After this marked decrease,
272 dissolved Ca^{2+} remained constant.

273 *G. lithophora* showed active growth during 792 h as shown by OD measurements
274 (Figure 2, right). During this period, OD reached a value of ~0.3, then a sharp decline in OD
275 was observed. Concomitantly, extracellular Ca^{2+} concentration remained constant and ^{226}Ra
276 in the soluble fraction decreased. The cause of this sharp decline in OD is unclear, but
277 possible reasons are presented later in the discussion (See Maximum uptake of ^{226}Ra and
278 ^{90}Sr in *G. lithophora)*. At the end of incubation (1392 h), 99 ± 5 % of initial ^{226}Ra was
279 removed from the solution.

280 **Retention mechanisms of ^{226}Ra and ^{90}Sr in *G. lithophora***

Here, we systematically tested different microbial processes to explain mechanism of ^{226}Ra and ^{90}Sr sequestration by *G. lithophora*. First, to distinguish adsorption to dead cells from other mechanisms, we compared uptake of ^{226}Ra and ^{90}Sr between living and dead cells of *G. lithophora*. The average uptake of ^{226}Ra in inactivated cell control, composed of dead cells of *G. lithophora*, was equal to 0.8 ± 0.1 µg (g of dry mass)$^{-1}$; in contrast the average ^{226}Ra uptake by active *G. lithophora* cells reached 3.9 ± 0.9 µg (g of dry mass)$^{-1}$ (Table 1~~Table 1~~). Likewise, the

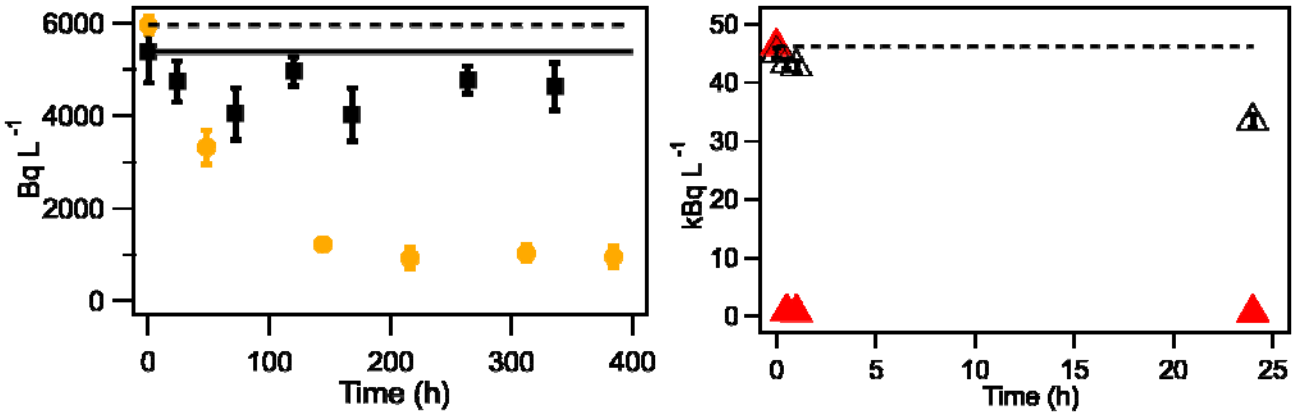

Figure 3: (Left) Time evolution of residual ^{226}Ra activity in the solution during growth of *G. lithophora* (●) and *Synechocystis* PCC 6803 (■) in BG-11. (Right) Time evolution of residual ^{90}Sr activity in high cell density suspensions (OD=0.5) of *G. lithophora* (▲) and *Synechocystis* PCC 6803 (Δ), both suspended in BG-11. The activity of ^{226}Ra added to BG-11 media is shown as dash line for *G. lithophora* cultures, and solid line for *Synechocystis* cultures. The activity of ^{90}Sr added to BG-11 media is shown as dash line for *G. lithophora* and *Synechocystis* cultures. Error bar shows ±σ.

average uptake of ^{90}Sr by dead *G. lithophora* cells was equal to 8.87 ± 0.2 ng (g of dry mass)$^{-1}$; in contrast the average ^{90}Sr uptake rate by active cells of *G. lithophora* measured 47.97 ± 1.5 ng (g of dry mass)$^{-1}$ (Table 1). Second, the relationship between biomineralization and sequestration of ^{226}Ra and ^{90}Sr was tested by comparing uptake of ^{226}Ra and ^{90}Sr by living cells of the non-biomineralizing *Synechocystis* and living cells of *G. lithophora*. The OD of *Synechocystis* during the incubation period is shown in Figure S1. Living cells of the non-biomineralizing *Synechocystis* retained 14 ± 2 % of ^{226}Ra in 336 h, while *G. lithophora* retained

83 ± 14 % of ^{226}Ra over the same duration (Figure 3). Similarly, incubation over 24 h of the non-biomineralizing *Synechocystis* at relatively high cell density (OD=0.5) retained 26 ± 1 % of ^{90}Sr, while *G. lithophora* retained 99.5 ± 10 % of the initial ^{90}Sr (Figure 3). While there could be differences in the cell surface composition between both strains, we argue that these differences are likely not substantial enough to induce 6 times more ^{226}Ra and 4 times more ^{90}Sr retention in *G. lithophora* than in *Synechocystis* PCC 6803. Altogether, these results suggest specific cellular processes are responsible for ^{226}Ra and ^{90}Sr retention by *G. lithophora.*

Table 1: Comparison of ^{226}Ra and ^{90}Sr uptake per unit biomass in different incubations

Sample ID	**^{226}Ra Retained* µg (g of dry mass)$^{-1}$**	**^{90}Sr retained** ng (g of dry mass)$^{-1}$**
Live *G. lithophora* cells	3.9 ± 0.9	47.9 ± 1.5
Dead *G. lithophora* cells	0.8 ± 0.1	8.87 ± 0.2

* mass uptake is average uptake during the first stage of Ra retention. The error bar shows ±σ
** mass uptake is average uptake when cells were exposed to 8.8 x 10^{-11} M of ^{90}Sr for 1 h.

Microbial processes of ^{226}Ra and ^{90}Sr sequestration can broadly be categorized into three groups: extracellular biomineralization, adsorption, and intracellular biomineralization[24]. Microbially induced extracellular biomineralization requires localized supersaturation of the solution with respect to Ca-carbonate phases. This results in precipitation of carbonate solids and ^{226}Ra and ^{90}Sr may co-precipitate within these

312 extracellular solids and be removed from the solution. Using Visual Minteq[38], we calculated
313 the saturation state of the solution with respect to Ca-carbonate phases to verify if this
314 mechanism was operational. Visual MINTEQ predicts that the experimental culture media
315 amended with ^{226}Ra and ^{90}Sr remained undersaturated with respect to Ca-carbonate phase(s)
316 (Figure S2- S3). Moreover, the state of solution undersaturation with respect to Ca-
317 carbonate solids is consistent with the observation that dissolved ^{226}Ra and ^{90}Sr activity
318 remained close to their initial activities in the abiotic control (Figure 1-2). Therefore,
319 extracellular precipitates of Ca-carbonate phases could not be a plausible sink of ^{226}Ra and
320 ^{90}Sr in our study.

321 One of the physicochemical processes that has been used widely for sequestering low
322 levels of contaminants from aqueous solutions is adsorption. Here, based on Figure 3 and
323 Table 1, adsorption of ^{226}Ra and ^{90}Sr at walls of culture flasks, at the cell surface and dead *G.*
324 *lithophora* biomass, removed 22% ^{226}Ra and 18% ^{90}Sr from solution, suggesting that
325 adsorption alone cannot reproduce the degree of ^{226}Ra and ^{90}Sr retained by *G. lithophora.*
326 The dissolved concentration of Ca^{2+} in ^{226}Ra uptake experiments by active cells of G.
327 lithophora was higher than the concentration of dissolved Ca^{2+} in the inactivated cell control
328 and the *Synechocystis* cultures. Because of competing effects for adsorption between Ca and
329 Ra, this implies that the degree of ^{226}Ra adsorption measured in the inactivated cell and by
330 *Synechocystis* controls was relatively overestimated compared to that in the presence of
331 active *G. lithophora* cells will likely be less in presence of excess Ca^{2+} furnished in ^{226}Ra
332 uptake experiments (Figure 2). Moreover, the cell normalized rate of uptake measured for
333 ^{90}Sr is consistent with those measured by Cam et al. for stable Sr isotope and shown to be
334 associated with intracellular uptake rather than adsorption[33]. These observations taken

335 altogether suggests that mechanism(s) other than adsorption are involved in ^{226}Ra and ^{90}Sr
336 uptake in *G. lithophora.*

337 Previously, TEM analyses of *G. lithophora* cells cultured in BG-11, amended with
338 high initial concentrations of stable Ba and Sr isotopes showed that most of the Sr and Ba
339 were sequestered within intracellular carbonates and to a lesser extent in intracellular
340 polyphosphates. Unfortunately, TEM analysis was not possible here to assess ^{226}Ra and ^{90}Sr
341 distribution within the cell because their concentrations were below the detection limits of
342 EDXS[39]. Nevertheless, considering ^{226}Ra and ^{90}Sr chemical affinities and similarity to Ca
343 and Ba, we propose that incorporation of ^{226}Ra and ^{90}Sr into intracellular carbonate (and
344 polyphosphate) inclusions is likely the primary mechanisms for their sequestration in *G.*
345 *lithophora*. It remains a mystery why *G. lithophora* would sequester radiotoxic ^{226}Ra and
346 ^{90}Sr elements within the cell. Unlike Ca, which is essential as a co-factor for cyanobacteria
347 in the photosystem II complex[40], there is no documented biological function of ^{226}Ra, ^{90}Sr or
348 Ba. Some studies have argued that trace amounts of non-essential elements can be
349 assimilated together with their corresponding essential analogues[24]. In fact, non-selective
350 transport of Sr^{2+} through cation channels have already been acknowledged by other
351 studies[41]. Hence, ^{226}Ra and ^{90}Sr could be "mistaken" for its chemical analog Ca, an essential
352 element, thereby resulting in their favorable uptake in *G. lithophora*. Alternatively, while
353 this is not ascertained by the present experiments, selective uptake of ^{226}Ra and ^{90}Sr by *G.*
354 *lithophora* should may also be considered because of two reasons: (1) Cam *et al*. showed
355 that *G. lithophora* selectively uptakes stable Sr over Ca[33]; (2) Uptake of ^{226}Ra and ^{90}Sr by *G.*
356 *lithophora* was not inhibited by Ca^{2+}, present at approximately 6 orders of magnitude higher
357 concentration than ^{226}Ra and ^{90}Sr. These observations favor involvement of another

biochemical process at play in *G. lithophora*. Typically, ion selectivity between similar ions such Sr, Ra, Ba, Ca requires an ion transport pathway to have some specific binding sites over at least part of its length. Future studies characterizing the affinity and specificity of various transporters involved in uptake of AEE in *G. lithophora* along with measurement of ^{90}Sr and ^{226}Ra uptake by *G. lithophora* at varying Ca: $^{90}Sr/^{226}Ra$ ratio may shed some light on molecular processes involved in uptake of ^{90}Sr and ^{226}Ra by *G. lithophora.*

Maximum uptake of ^{226}Ra and ^{90}Sr by *G. lithophora*

Understanding the maximum uptake capacity of ^{226}Ra and ^{90}Sr by *G. lithophora* is an important criterion for its assessment as a potential bioremediation strategy. The maximum radionuclide uptake capacity by a microorganism is an elusive concept as a zero net uptake rate doesn't always signal maximum uptake capacity. For example, net uptake may appear to cease when the amount of radionuclide added to the solution is exhausted before the cells reach their maximum uptake capacity. In the case of ^{226}Ra, the total ^{226}Ra accumulated in *G. lithophora* over the total duration of incubation equals to 133 kBq (g of dry mass)$^{-1}$ (Figure 2 and Table1). The OD decline after 792 h may possibly indicate cell lysis and/or cell aggregation, settling and/or attachment of cells to the flasks. Visual inspection of the cultures after 792 h did reveal some aggregation and settling of the cells (data no shown). The decrease in the uptake of ^{226}Ra during the 2nd stage may signal that the cells have reached maximum ^{226}Ra uptake capacity. To test whether this is the case, cultures of *G. lithophora* were grown in BG-11 containing ^{226}Ra at a concentration 25 times higher than the experiment here. The high ^{226}Ra concentration experiments showed that over 30 days 70% of ^{226}Ra was removed and 962 kBq (g of biomass)$^{-1}$ ^{226}Ra sequestered by *G. lithophora* (Figure S4). This implies that the decrease in ^{226}Ra uptake rate during 2nd stage is not

because cells reached maximum uptake capacity but for some other reasons yet to be discovered. Similar to ^{226}Ra, total ^{90}Sr accumulated by *G. lithophora* in 24 h was equal to 250 kBq (g of biomass)$^{-1}$(Figure 1 and Table1). To test whether this amount of ^{90}Sr sequestered was equal to maximum uptake capacity, culture of *G. lithophora* at high cell density were successively spiked with ^{90}Sr and uptake of ^{90}Sr measured in the supernatant. The multiple spike experiments showed that 924 kBq (g of biomass)$^{-1}$ was incorporated within *G. lithophora* over 24 hr (Figure S5). After 24 h, no further ^{90}Sr accumulation was measured as the cells exhausted the amount of ^{90}Sr provided. Together, these observations suggest that in the present study, measured ^{226}Ra and ^{90}Sr accumulation by *G. lithophora* is a lower estimate of its maximum uptake capacity.

Environmental Implications and Bioremediation

Both uptake capacity and selectivity play an important feature for assessment of an organism's effectiveness for ^{90}Sr and ^{226}Ra remediation. Tables 2 and 3 compare ^{90}Sr and ^{226}Ra uptake capacity of *G. lithophora* with other organisms known to uptake ^{90}Sr or ^{226}Ra. For the screened bioremediation candidates, uptake capacities of ^{90}Sr and ^{226}Ra are reported assuming ideal conditions, *i.e*. in absence of Ca and other divalent ions. Such conditions are not representative of environments contaminated with ^{90}Sr and ^{226}Ra, which contain excess Ca and/or other divalent ions. Presence of Ca and other divalent ions in the solution may compromise the uptake of ^{226}Ra and ^{90}Sr. For example, 40% of ^{90}Sr was removed by *Vetiveria zizanoids* from solution containing Ca/^{90}Sr molar ratio of 3.6 x 10^6, while 94% removal was achieved in absence of Ca[42]. In another example, *Calotropis gigantea* exhibited high accumulation of ^{90}Sr (104 ng g^{-1}) but from a solution containing only ^{90}Sr[43].

403 Whether the high ^{90}Sr removal efficiency of *C. gigantea* is maintained within an
404 environmentally relevant matrix remains unknown. In the case of ^{226}Ra, the uptake exhibited
405 by dead biomass was achieved under conditions where ^{226}Ra was the only AEE present and
406 therefore unlikely to be replicated in the environment to the same extent. Therefore, the
407 current bioremediation strategies listed in Table 2-3 are inadequate in efficiently achieving
408 selective removal of ^{226}Ra and ^{90}Sr in the presence of Ca.

409 **Table 2:** Comparison of ^{226}Ra uptake by *G. lithophora* with previously reported experimental data on ^{226}Ra
410 uptake by organisms.

	Radium Uptake
Dead Biomass	**(µg g^{-1})**
P. fluorescens[44]	0.02
Streptomycene nives[44]	0.58
Activated sludge[44]	0.075
Activated sludge[45]	0.04
N. carneum[25]	1.3
N. insulare[25]	1.2
O. geminata[25]	1.35
S. laxissima[25]	1.3
Serratia sp. ZF03[45]	1.03
P. chrysogenum[46]	0.076
G. emersonii[47]	1.86
Live Biomass	
D. linearis[48]	4.5
*G. lithophora (this study)**	26.1

* based on *G. lithophora grown in elevated ^{226}Ra activity in a preliminary experiment (Figure S4)*

411

412 On the other hand, *G. lithophora* exhibits highest uptake of ^{90}Sr and ^{226}Ra among all
413 the active and dead microorganisms. Since OD values in experiments using ^{90}Sr were
414 measured under the same conditions and setup as in Cam et al[36], their conversion to cell
415 numbers and cell mass are expected to be correct. Alternatively, we note that quantity of
416 ^{226}Ra sequestered per unit biomass of *G. lithophora* cells might be approximate estimations

only because presence of ^{226}Ra during growth of *G. lithophora* may induce physiological changes and alter the previously reported relationship between OD, cell density, and cell mass[36].Unlike previously reported uptake studies, *G. lithophora* uptakes ^{90}Sr and ^{226}Ra in presence of excess Ca- initial molar ratio of Ca/^{90}Sr and Ca/^{226}Ra of the cultures equal $2.3x10^6$ and $1.2x10^6$ respectively. Interestingly, ^{226}Ra accumulation by *G. lithophora's* overwhelmingly exceeds ^{226}Ra uptake capacity of *Dicranopteris linearis*, identified as a ^{226}Ra hyper-accumulator[48]. The remarkable ability of *G. lithophora* to retain high activities of ^{226}Ra and ^{90}Sr in comparison with other organisms makes it an attractive candidate for bioremediation applications in decontamination of low salinity radioactive wastewater streams. Such a strategy could be envisioned as an *ex-situ* treatment, integrated (e.g. as a bioreactor) within an existing wastewater treatment plant. Compared to *G. lithophora,* other ^{90}Sr/^{226}Ra bioremediation candidates are mostly plants (Table2-3). There are practical considerations of using cyanobacterium *G. lithophora* vs. plants for bioremediation, such as harvesting of biomass, growth times, duration of decontamination and treatment of radioactive biomass. A complete development of *G. lithophora* based bioremediation would require determining these aspects in future studies.

Table 3: Comparison of Sr uptake in *G. lithophora* with previously reported experimental data on ^{90}Sr uptake by organisms

	Uptake capacity (ng g^{-1})	**% removal**
Organism		
V. zizanoides (0mM Ca)[42]	-	94%
V. zizanoides (40 mM Ca)[42]	-	40%
Paspalum notatum[49]**	0.14	20%
Sorghum halense[49]**	0.14	32%
Panicum virginatum[49]**	0.15	23%
Amaranthus retoflexus[50]	0.000077	5%
Calotropis gigantea[43]*	103.37	97%
G. lithophora (this study)$^{+}$	177	99%

* Uptake achieved in 168 h

** Concentration in plant tissue after 8 weeks of harvest

$^{+}$ Based on multi-spike experiment (Figure S5)

Another aspect of bioremediation of radionuclides in the environment is the ability of microorganism to survive in the presence of ionizing radiation. The intracellular uptake of radiotoxic ^{226}Ra and ^{90}Sr could potentially result in oxidative damage in DNA, proteins and lipids due to the generation of reactive oxygen species. Cyanobacteria have been detected in radioactive areas surrounding Chernobyl nuclear reactor[51], uranium mining operations [52] and in vicinity of hydrothermal spring caves[53], suggesting that they may have some degree of resistance to ionizing radiation. However, little is known about *G. lithophora*'s radiotolerance and response to oxidative stress and future experiments characterizing the viability of *G. lithophora* cells when exposed to elevated radiation could provide some insights in this regard.

G. lithophora sequesters ^{226}Ra and ^{90}Sr within intracellular ACC inclusions at very low extracellular Ra/Ca concentration ratios, offering a unique solution to the general problem of remediating ^{226}Ra and ^{90}Sr in aqueous environments with naturally high Ca concentrations. Further studies investigating the stability of intracellular inclusions in environmentally relevant matrices and optimization of various process parameters such as maximum ^{226}Ra and ^{90}Sr uptake capacity, and tolerance to other metalloids present in the waste streams will be needed to ensure successful development of *G. lithophora* based bioremediation approach for ^{90}Sr and ^{226}Ra.

4. ASSOCIATED CONTENT

This manuscript is accompanied by Supporting Information. An extra document contains 5 figures. Data on OD of cultures in absence of radionuclide, saturation indices of Ca and Sr solids in the solution, ^{226}Ra uptake by *G. lithophora* from BG-11 containing 210 kBq L^{-1} ^{226}Ra, and data on uptake of ^{90}Sr by *G. lithophora* during successive spike experiment.

458 5. ACKNOWLEDGMENTS

459 We would like to thank Timothy McClure (MIT) for his assistance with ICP-OES,
460 Ryan Samz and Mitchell S Galanek, MIT Environmental Health and Safety, for supplying
461 ^{226}Ra stock solutions, radiation protection equipment and safety expertise. We thank Fériel
462 Skouri-Panet and Margot Coutaud (IMPMC) for assistance in the Sr experiments. The
463 authors declare no competing financial interest.

464

465

466

467 **REFERENCE**

468 (1) Hutchins, D.; Mulholland, M.; Fu, F. Nutrient Cycles and Marine Microbes in a CO2-
469 Enriched Ocean. *Oceanography* **2009**, *22* (4), 128–145.

470 (2) Riding, R. Cyanobacterial Calcification, Carbon Dioxide Concentrating Mechanisms,
471 and Proterozoic-Cambrian Changes in Atmospheric Composition. *Geobiology* **2006**, *4*
472 (4), 299–316.

473 (3) Benzerara, K.; Skouri-Panet, F.; Li, J.; Ferard, C.; Gugger, M.; Laurent, T.;
474 Couradeau, E.; Ragon, M.; Cosmidis, J.; Menguy, N.; Margaret-Oliver, I.; Tavera, R.;
475 Lopez-Garcia, P.; Moreira, D. Intracellular Ca-Carbonate Biomineralization Is
476 Widespread in Cyanobacteria. *Proc. Natl. Acad. Sci.* **2014**, *111* (30).

477 (4) Couradeau, E.; Benzerara, K.; Gérard, E.; Moreira, D.; Bernard, S.; Brown, G. E. J.;
478 López-García, P. An Early-Branching Microbialite Cyanobacterium Forms
479 Intracellular Carbonates. *Science.* **2012**, *336*, 459–462.

480 (5) De Wever, A.; Benzerara, K.; Gugger, M.; Coutaud, M.; Caumes, G.; Poinsot, M.;
481 Skouri, F.; Thierry, P.; Elodie, L. Evidence of High Ca Uptake by Cyanobacteria
482 Forming Intracellular CaCO 3 and Impact on Their Growth. *Geobiology* **2019**, 1–15.

483 (6) Li, J.; Margaret Oliver, I.; Cam, N.; Boudier, T.; Blondeau, M.; Leroy, E.; Cosmidis,

J.; Skouri-Panet, F.; Guigner, J.-M.; Férard, C.; Poinsot, M.; Moreira, D.; Lopez-Garcia, P.; Cassier-Chauvat, C.; Chauvat, F.; Benzerara, K. Biomineralization Patterns of Intracellular Carbonatogenesis in Cyanobacteria: Molecular Hypotheses. *Minerals* **2016**, *6* (1), 10.

(7) Szabo, Z.; dePaul, V. T.; Fischer, J. M.; Kraemer, T. F.; Jacobsen, E. Occurrence and Geochemistry of Radium in Water from Principal Drinking-Water Aquifer Systems of the United States. *Appl. Geochemistry* **2012**, *27* (3), 729–752.

(8) United States Environmental Protection Agency. *Radionuclides Rule _ Drinking Water Requirements for States and Public Water Systems _ US EPA*.

(9) International Atomic Energy Agency (IAEA). The Environmental Behaviour of Radium: Revised Edition. *Tech. Reports Ser. No. 476* **2014**, No. 476, 44–51.

(10) United States Nuclear Regulatory Commission. NRC: 10 CFR Part 20 - Appendix B - Radionuclide Table - Cesium-137. 2017.

(11) Warner, N. R.; Cidney, C. A.; Jackson, R. B.; Vengosh, A. Impacts of Shale Gas Wastewater Disposal on Water Quality in Western PA. *Environ. Sci. Technol.* **2013**, 1–14.

(12) Chellam, S.; Clifford, D. A. Physical-Chemical Treatment of Groundwater Contaminated by Leachate from Surface Disposal of Uranium Tailings. *J. Environ. Eng.* **2002**, *128* (10), 942–952.

(13) Casacuberta, N.; Masqué, P.; Garcia-Orellana, J.; Garcia-Tenorio, R.; Buesseler, K. O. 90Sr and 89Sr in Seawater off Japan as a Consequence of the Fukushima Dai-Ichi Nuclear Accident. *Biogeosciences* **2013**, *10* (6), 3649–3659.

(14) Vakulovsky, S. M.; Nikitin, A. I.; Chumichev, V. B.; Katrich, I. Y.; Voitsekhovich, O. A.; Medinets, V. I.; Pisarev, V. V.; Bovkum, L. A.; Khersonsky, E. S. Cesium-137 and Strontium-90 Contamination of Water Bodies in the Areas Affected by Releases from the Chernobyl Nuclear Power Plant Accident: An Overview. *J. Environ. Radioact.* **1994**, *23* (2), 103–122.

(15) Povinec, P. P.; Hirose, K.; Aoyama, M. Radiostrontium in the Western North Pacific:

512 Characteristics, Behavior, and the Fukushima Impact. *Environ. Sci. Technol.* **2012**, *46*
513 (18), 10356–10363.

514 (16) Idaho National Engineering Laboratory, I. Selected Radionuclides Important to Low-
515 Level Radioactive Waste Management. **1996**, No. November, 1–413.

516 (17) Pagnanelli, F.; Papini, M. P.; Toro, L.; Trifoni, M.; Vegliò, F. Biosorption of Metal
517 Ions on Arthrobacter Sp.: Biomass Characterization and Biosorption Modeling.
518 *Environ. Sci. Technol.* **2000**, *34* (13), 2773–2778.

519 (18) Volesky, B. Detoxification of Metal-Bearing Effluents: Biosorption for the next
520 Century. *Hydrometallurgy* **2001**, *59* (2–3), 203–216.

521 (19) Brower, J. B.; Ryan, R. L.; Pazirandeh, M. Comparison of Ion-Exchange Resins and
522 Biosorbents for the Removal of Heavy Metals from Plating Factory Wastewater.
523 **1997**, *31* (10), 2910–2914.

524 (20) Lloyd, J. R.; Renshaw, J. C. Bioremediation of Radioactive Waste: Radionuclide-
525 Microbe Interactions in Laboratory and Field-Scale Studies. *Curr. Opin. Biotechnol.*
526 **2005**, *16*, 254–260.

527 (21) Gadd, G. M. Metals, Minerals and Microbes: Geomicrobiology and Bioremediation.
528 *Microbiology* **2010**, *156* (3), 609–643.

529 (22) Ruggiero, C. E.; Boukhalfa, H.; Forsythe, J. H.; Lack, J. G.; Hersman, L. E.; Neu, M.
530 P. Actinide and Metal Toxicity to Prospective Bioremediation Bacteria. *Environ.*
531 *Microbiol.* **2005**, *7* (1), 88–97.

532 (23) Tsezos, M.; Keller, D. M. Adsorption of Radium-226 by Biological Origin
533 Absorbents. *Biotechnol. Bioeng.* **1983**, *25* (1), 201–215.

534 (24) Newsome, L.; Morris, K.; Lloyd, J. R. The Biogeochemistry and Bioremediation of
535 Uranium and Other Priority Radionuclides. *Chem. Geol.* **2014**, *363*, 164–184.

536 (25) Pohl, P.; Schimmack, W. Adsorption of Radionuclides (134Cs, 85Sr, 226Ra, 241Am)
537 by Extracted Biomasses of Cyanobacteria (Nostoc Carneum, N. Insulare, Oscillatoria
538 Geminata and Spirulina Laxis-Sima) and Phaeophyceae (Laminaria Digitata and L.

539 Japonica; Waste Products from Alginat. *J. Appl. Phycol.* **2006**, *18* (2), 135–143.

540 (26) Satvatmanesh, D.; Siavoshi, F.; Beitollahi, M. M.; Amidi, J.; Fallahian, N.
541 Biosorption of 226Ra in High Level Natural Radiation Areas of Ramsar, Iran. *J.*
542 *Radioanal. Nucl. Chem.* **2003**, *258* (3), 483–486.

543 (27) Liu, M.; Dong, F.; Kang, W.; Sun, S.; Wei, H.; Zhang, W.; Nie, X.; Guo, Y.; Huang,
544 T.; Liu, Y. Biosorption of Strontium from Simulated Nuclear Wastewater by
545 Scenedesmus Spinosus under Culture Conditions: Adsorption and Bioaccumulation
546 Processes and Models. *Int. J. Environ. Res. Public Health* **2014**, *11* (6), 6099–6118.

547 (28) Fukuda, S. ya; Iwamoto, K.; Atsumi, M.; Yokoyama, A.; Nakayama, T.; Ishida, K.
548 ichiro; Inouye, I.; Shiraiwa, Y. Global Searches for Microalgae and Aquatic Plants
549 That Can Eliminate Radioactive Cesium, Iodine and Strontium from the Radio-
550 Polluted Aquatic Environment: A Bioremediation Strategy. *J. Plant Res.* **2014**, *127*
551 (1), 79–89.

552 (29) Krejci, M. R.; Finney, L.; Vogt, S.; Joester, D. Selective Sequestration of Strontium in
553 Desmid Green Algae by Biogenic Co-Precipitation with Barite. *ChemSusChem* **2011**,
554 *4* (4), 470–473.

555 (30) Lee, S. Y.; Jung, K. H.; Lee, J. E.; Lee, K. A.; Lee, S. H.; Lee, J. Y.; Lee, J. K.; Jeong,
556 J. T.; Lee, S. Y. Photosynthetic Biomineralization of Radioactive Sr via Microalgal
557 CO2absorption. *Bioresour. Technol.* **2014**, *172*, 449–452.

558 (31) Achal, V.; Pan, X.; Zhang, D. Bioremediation of Strontium (Sr) Contaminated
559 Aquifer Quartz Sand Based on Carbonate Precipitation Induced by Sr Resistant
560 Halomonas Sp. *Chemosphere* **2012**, *89* (6), 764–768.

561 (32) Lauchnor, E. G.; Schultz, L. N.; Bugni, S.; Mitchell, A. C.; Cunningham, A. B.;
562 Gerlach, R. Bacterially Induced Calcium Carbonate Precipitation and Strontium
563 Coprecipitation in a Porous Media Flow System. *Environ. Sci. Technol.* **2013**, *47* (3),
564 1557–1564.

565 (33) Cam, N.; Benzerara, K.; Georgelin, T.; Jaber, M.; Lambert, J. F.; Poinsot, M.; Skouri-
566 Panet, F.; Cordier, L. Selective Uptake of Alkaline Earth Metals by Cyanobacteria

Forming Intracellular Carbonates. *Environ. Sci. Technol.* **2016**, *50* (21), 11654–11662.

(34) Bailey, S.; Grossman, A. Photoprotection in Cyanobacteria: Regulation of Light Harvesting. *Photochem. Photobiol.* **2008**, *84* (6), 1410–1420.

(35) Ragon, M.; Benzerara, K.; Moreira, D.; Tavera, R.; Lopez-Garcia, P. 16S RDNA-Based Analysis Reveals Cosmopolitan Occurrence but Limited Diversity of Two Cyanobacterial Lineages with Contrasted Patterns of Intracellular Carbonate Mineralization. *Front. Microbiol.* **2014**, *5*, 1–11.

(36) Moreira, D.; Tavera, R.; Benzerara, K.; Skouri-Panet, F.; Couradeau, E.; Gérard, E.; Fonta, C. L.; Novelo, E.; Zivanovic, Y.; López-García, P. Description of Gloeomargarita Lithophora Gen. Nov., Sp. Nov., a Thylakoid-Bearing, Basal-Branching Cyanobacterium with Intracellular Carbonates, and Proposal for Gloeomargaritales Ord. Nov. *Int. J. Syst. Evol. Microbiol.* **2017**, *67* (3), 653–658.

(37) Stanier, R. Y.; Deruelles, J.; Rippka, R.; Herdman, M.; Waterbury, J. B. Generic Assignments, Strain Histories and Properties of Pure Cultures of Cyanobacteria. *Microbiology* **1979**, *111* (1), 1–61.

(38) Gustafsson, J. P. Visual MINTEQ 3.0 User Guide. *Dep.of L. Water Resour.eng* **2012**, 1–73.

(39) Blondeau, M.; Benzerara, K.; Ferard, C.; Guigner, J. M.; Poinsot, M.; Coutaud, M.; Tharaud, M.; Cordier, L.; Skouri-Panet, F. Impact of the Cyanobacterium Gloeomargarita Lithophora on the Geochemical Cycles of Sr and Ba. *Chem. Geol.* **2018**, *483*, 88–97.

(40) Debus, R. J. The Manganese and Calcium Ions of Photosynthetic Oxygen Evolution. *Biochem. Biophys. Acta* **1992**, *1102* (3), 269–352.

(41) Gupta, D. K.; Schulz, W.; Steinhauser, G.; Walther, C. Radiostrontium Transport in Plants and Phytoremediation. *Environ. Sci. Pollut. Res.* **2018**, *25* (30), 29996–30008.

(42) Singh, S.; Eapen, S.; Thorat, V.; Kaushik, C. P.; Raj, K.; D'souza, S. Phytoremediation of 137cesium and 90strontium from Solutions and Low-Level

595 Nuclear Waste by Vetiveria Zizanoides. *Exotoxicology Enviornmental Saf.* **2008**, *69*,
596 306–311.

597 (43) Eapen, S.; Singh, S.; Thorat, V.; Kaushik, C. P.; Raj, K.; D'Souza, S. F.
598 Phytoremediation of Radiostrontium (90 Sr) and Radiocesium (137 Cs) Using Giant
599 Milky Weed (Calotropis Gigantea R.Br.) Plants. *Chemosphere* **2006**, *65* (11), 2071–
600 2073.

601 (44) Tsezos, M.; Keller, D. M. Adsorption of Radium-226 by Biological Origin
602 Absorbents. *Biotechnol. Bioeng.* **1983**, *25*, 201–215.

603 (45) Zakeri, F.; Noghabi, K. A.; Sadeghizadeh, M.; Kardan, M. R.; Masoomi, F.;
604 Farshidpour, M. R.; Atarilar, A. Serratia Sp. ZF03: An Efficient Radium Biosorbent
605 Isolated from Hot-Spring Waters in High Background Radiation Areas. *Bioresour.*
606 *Technol.* **2010**, *101* (23), 9163–9170.

607 (46) IAEA. Various. *Treat. Liq. Effl. from uranium mines mills* **2004**, No. October, 246 p.

608 (47) Heidari, F.; Riahi, H.; Aghamiri, M. R.; Shariatmadari, Z.; Zakeri, F. Isolation of an
609 Efficient Biosorbent of Radionuclides (226Ra,238U): Green Algae from High-
610 Background Radiation Areas in Iran. *J. Appl. Phycol.* **2017**, *29* (6), 2887–2898.

611 (48) Chao, J. H.; Chuang, C. Y. Accumulation of Radium in Relation to Some Chemical
612 Analogues in Dicranopteris Linearis. *Appl. Radiat. Isot.* **2011**, *69* (1), 261–267.

613 (49) Entry, J. A.; Watrud, L. S.; Reeves, M. Influence of Organic Amendments on the
614 Accumulation of 137Cs and 90Sr from Contaminated Soil by Three Grass Species.
615 *Water. Air. Soil Pollut.* **2001**, *126* (3–4), 385–398.

616 (50) Fuhrmann, M.; Lasat, M. M.; Ebbs, S. D.; Kochian, L. V.; Cornish, J. Uptake of
617 Cesium-137 and Strontium-90 from Contaminated Soil by Three Plant Species;
618 Application to Phytoremediation. *J. Environ. Qual.* **2017**, *31* (3), 904.

619 (51) Ragon, M.; Restoux, G.; Moreira, D.; Møller, A. P.; López-García, P. Sunlight-
620 Exposed Biofilm Microbial Communities Are Naturally Resistant to Chernobyl
621 Ionizing-Radiation Levels. *PLoS One* **2011**, *6* (7).

(52) Lusa, M.; Knuutinen, J.; Lindgren, M.; Virkanen, J.; Bomberg, M. Microbial Communities in a Former Pilot-Scale Uranium Mine in Eastern Finland – Association with Radium Immobilization. *Sci. Total Environ.* **2019**, *686*, 619–640.

(53) Enyedi, N. T.; Anda, D.; Borsodi, A. K.; Szabó, A.; Pál, S. E.; Óvári, M.; Márialigeti, K.; Kovács-Bodor, P.; Mádl-Szőnyi, J.; Makk, J. Radioactive Environment Adapted Bacterial Communities Constituting the Biofilms of Hydrothermal Spring Caves (Budapest, Hungary). *J. Environ. Radioact.* **2019**, *203* (March), 8–17.

Sequestration of radionuclides Radium-226 and Strontium-90 by cyanobacteria forming intracellular calcium carbonates

Neha Mehta[1], Karim Benzerara[2], Benjamin D. Kocar[1,3*], Virginie Chapon[4]

[1,3] Department of Civil and Environmental Engineering, Massachusetts Institute of Technology, Cambridge, Massachusetts 02139, United States

[2] Sorbonne Université, Muséum National d'Histoire Naturelle, UMR CNRS 7590, Institut de Minéralogie, de Physique des Matériaux et de Cosmochimie, IMPMC, 75005 Paris, France

[3.] Exponent, Inc. 1055 E. Colorado Blvd, Suite 500. Pasadena, California 91106, United States.

[4] CEA, CNRS, Aix-Marseille Université, UMR 7265 Biosciences and Biotechnologies Institute of Aix-Marseille, 13108 Saint-Paul-lez-Durance, France.

*Corresponding Author

4 Pages; 5 figures

Figure S1: Time evolution of OD (circles) of *Synechocystis* PCC 6803 cultures in BG-11 in triplicate.

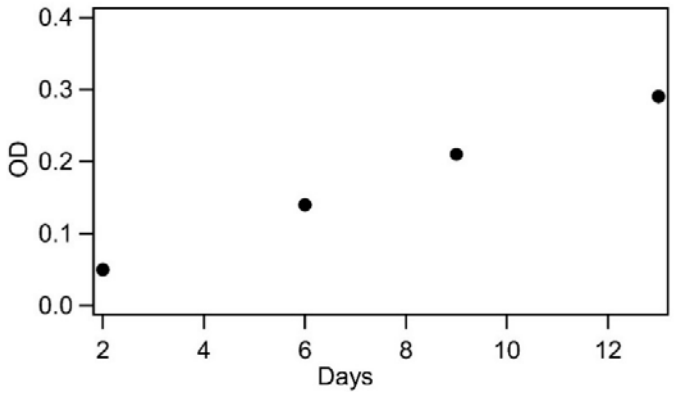

Saturation Indices calculation:

Visual MINTEQ (3.0) software package was used to calculate saturation indices of the culture medium with several possible Ca and Sr solids based on the bulk chemical analyses. The cultures were assumed to be in free exchange with the atmosphere with a partial CO_2 pressures of 3.5 atm. Using multi-sweep analysis, saturation indices were calculated for all Ca-carbonate phases reported in the Visual MINTEQ database as a function of dissolved Ca concentration at fixed pH of 8, for cultures amended with ^{226}Ra. In contrast, saturation indices for all Ca and Sr solids reported in Visual MINTEQ database were calculated as a function of pH and fixed dissolved Ca^{2+} for cultures amended with ^{90}Sr.

Figure S2: The saturation indices of the solution with Ca-carbonate solids that may possibly remove ^{226}Ra are plotted as a function of dissolved total Ca concentration (at fixed pH=8)

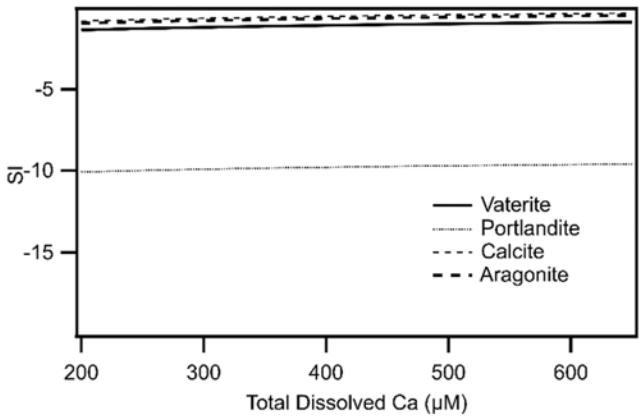

Figure S3: The saturation indices of the solution with Ca and Sr carbonate solids that may possibly remove ^{90}Sr from solution, are plotted as a function of solution pH (at fixed total dissolved Ca^{2+}=250 μM).

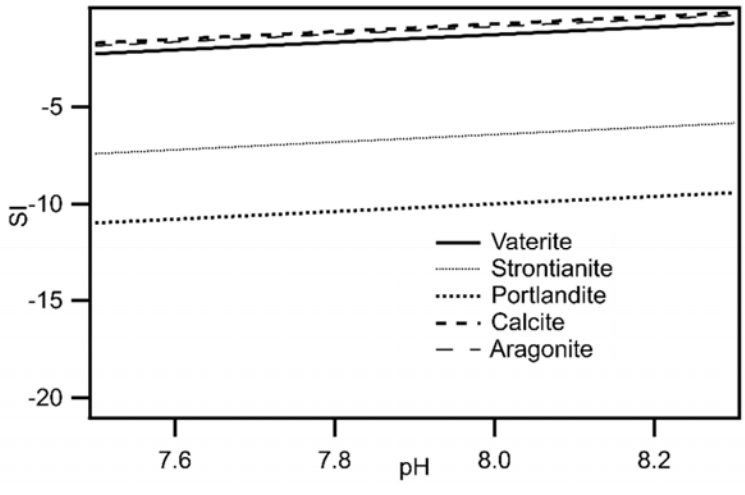

Figure S4: Cell grown in BG-11 amended with 210 kBq L^{-1} ^{226}Ra, and $6.32x10^{-4}$ M Ca. The squares denote residual ^{226}Ra activity in the solution and circles denote OD of the cell suspension.

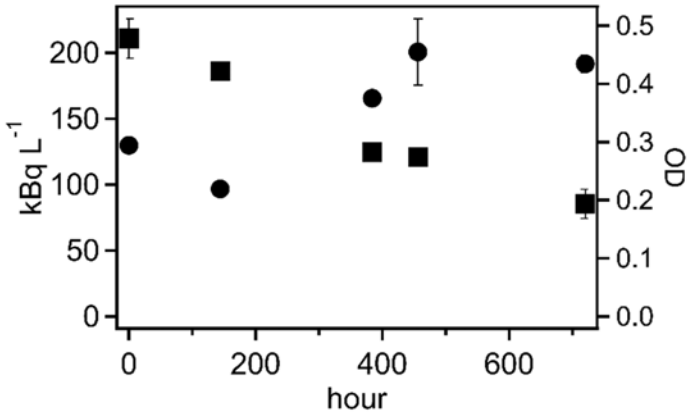

Figure S5: *G. lithophora* cells suspended at OD=0.5 in BG-11 amended with ^{90}Sr. The BG-11 was successively spiked with ^{90}Sr to measure maximum uptake of ^{90}Sr by *G. lithophora.* The total amount of ^{90}Sr uptake measured 160 $kBqL^{-1}$ (40 $kBqL^{-1}$ per spike), which considering an OD of 0.5 equals to 924 kBq $(g\ of\ biomass)^{-1}$